Efficient Channeling of Fluorescence Photons from Single Quantum Dots into Guided Modes of Optical Nanofiber

Ramachandrarao Yalla,[1] Fam Le Kien,[1] M. Morinaga,[2] and K. Hakuta[1]
[1]Center for Photonic Innovations, University of Electro-Communications, Chofu, Tokyo 182-8585, Japan
[2]Institute for Laser Science, University of Electro-Communications, Chofu, Tokyo 182-8585, Japan
(Received 9 April 2012; published 8 August 2012)

We experimentally demonstrate the efficient channeling of fluorescence photons from single q dots on optical nanofiber into the guided modes by measuring the photon-count rates through the guided and radiation modes simultaneously. We obtain the maximum channeling efficiency to be 22.0($\pm$4.8)% at a fiber diameter of 350 nm for the emission wavelength of 780 nm. The results may open new possibilities in quantum information technologies for generating single photons into single-mode optical fibers.

DOI: 10.1103/PhysRevLett.109.063602 PACS numbers: 42.50.Ct, 42.50.Ex, 42.50.Pq, 78.67.Hc

Efficient collection of fluorescence photons from a single emitter into a single-mode fiber is a major challenge in the context of quantum information science. For that purpose various novel techniques have been proposed so far. The examples would include micropillar cavities [1], photonic crystal cavities [2], solid immersion lens [3], and plasmonic metal nanowires [4]. However, in these techniques, the subsequent coupling of fluorescence photons into a single-mode fiber may reduce the actual collection efficiency. In the view of the ability to directly couple fluorescence photons into a single-mode fiber, tapered optical fibers with submicron diameter, termed as optical nanofibers, would be particularly promising. It has been theoretically predicted that, by positioning the emitter on the nanofiber surface, one can channel the fluorescence photons into the nanofiber-guided modes with an efficiency higher than 20% [5,6], and moreover, fibers can be tapered adiabatically to keep the light transmission into the single-mode fiber higher than 90% [7,8].

In the last decade, optical nanofibers have been attracting considerable attention in the field of quantum optics. Many works have been reported so far using laser-cooled atoms. Channeling of fluorescence photons into the guided modes has been demonstrated [7], and photon correlations from single atoms have been measured systematically through nanofiber-guided modes [9,10]. Fluorescence emission spectrum has been measured for few atoms through the guided mode by combining optical-heterodyne and photon-correlation methods [11]. Various schemes have been proposed for trapping atoms around the nanofiber [12–14], and the trapping has been experimentally demonstrated [15] using dipole-trapping method via two-color laser fields [13]. However, the channeling efficiency of fluorescence photons into the guided modes has not been measured yet, although the works so far imply a reasonable correspondence to the theoretical predictions [7]. One reason would be due to a fact that atoms are not on the nanofiber surface and the atom-surface distance could not be estimated accurately.

Recently, two groups have reported the photon-counting measurements from semiconductor q dots deposited on nanofibers [16,17]. They absolutely measured the photon-count rates into the guided modes for one q dot. They discussed the channeling efficiency of fluorescence photons into the guided modes based on the measured results. However, as pointed out in Ref. [17], the value which can be obtained from such measurements is not the channeling efficiency itself, but is a product of the channeling efficiency and the quantum efficiency of the q dot. Therefore, the channeling efficiency cannot be determined from the measurements without accurate information on the quantum efficiency for the one q dot which is measured.

In this Letter, we experimentally determine the channeling efficiency of fluorescence photons from single q dots on optical nanofiber into the guided modes. We measure the photon-count rates through the guided and radiation modes simultaneously for various diameters of nanofiber. The measured results completely reproduce the theoretical predictions [5,6] within the experimental errors. The maximum channeling efficiency we obtained was 22.0($\pm$4.8)% at the fiber diameter of 350 nm for the emission wavelength of 780 nm.

Figure 1 illustrates the schematic diagram of the experimental setup. Main part of the set up consists of inverted microscope (Eclipse Ti-U, Nikon) with a computer-controlled x-y stage, optical nanofiber, and subpicoliter needle dispenser (ND-2000, Applied Micro Systems). Optical nanofiber is placed on the x-y stage to precisely control the nanofiber position to the focus point of the microscope. Optical nanofibers are produced by adiabatically tapering commercial single-mode optical fibers (SMF1, cutoff wavelength: 1.3 μm) using a heat and pull technique. The diameter of nanofiber is measured using a scanning electron microscope before and after the optical experiments. The thinnest diameter of the nanofiber is 300–400 nm, and the nanofiber diameter varies along the fiber axis by 100 nm/1 mm. Ambiguity of the diameter measurements is estimated to be 6%. The transmission through the optical nanofiber is

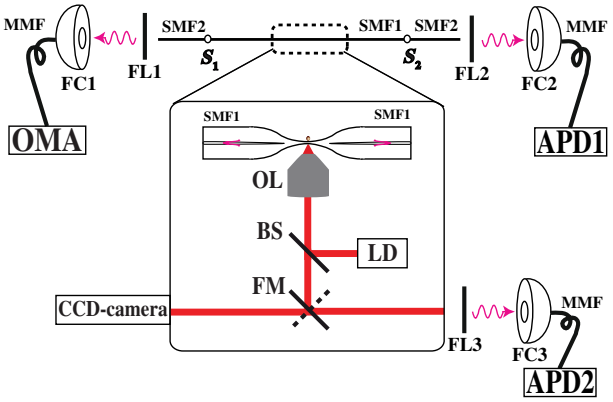

FIG. 1 (color online). Schematic diagram of the experimental setup. Inset shows the optical nanofiber and microscope system. OL, BS, FM, and FL denote objective lens, beam splitter, flipper mirror, and filter, respectively. SMF, FC, and MMF denote single-mode fiber, fiber coupler, and multimode fiber, respectively. LD, APD, and OMA denote laser diode, avalanche photodiode, and optical multichannel analyzer, respectively.

measured to be 90% using a fiber-coupled superluminescence light emitting diode (SLED) at 800 nm.

We use core–shell type colloidal CdSeTe (ZnS) q dots having emission wavelength at 790 nm (Q21371MP, Invitrogen). We use the subpicoliter needle dispenser to deposit q dots on nanofibers. The dispenser consists of a tapered glass tube which contains diluted q-dot solution and a needle having a tip of diameter 17 μm. The needle axis is adjusted to coincide with the axis of the microscope, and the needle-tip position is computer controlled along the axis. Once the needle tip passes through the tapered glass tube, it carries a small amount of q-dot solution at its edge. In order to deposit q dots on nanofiber with minimum scattering loss, the needle-tip position is adjusted so that the q-dot solution at its tip just touches the nanofiber surface. Note that this method could deposit q dots only on the upper surface of nanofiber. The deposition is done for several positions along the fiber axis corresponding to the fiber diameter of 300–800 nm. The transmission through the optical nanofibers is dropped to 81% after the depositions. The depositions are done for three optical nanofiber samples, and the following measurements are carried out for all the deposited positions.

The q dots are excited using continuous wave laser diode (LD) at a wavelength of 640 nm. The excitation beam is focused to the nanofiber by the microscope objective lens (OL) [40 ×, numerical aperture (NA) = 0.6]. Regarding the fluorescence photons channeled into the guided modes, in order to guarantee the observation through the fundamental mode (HE_{11}), SMF1 is fusion spliced to another single-mode fiber SMF2 (cutoff wavelength: 557 nm) at both ends, marked as S_1, S_2 in Fig. 1. Each end of SMF2 is angle polished to avoid the effect of reflection. The fluorescence light beam from each end of SMF2 is filtered from the scattered excitation laser light with a color glass filter FL1 (FL2) (R72, HOYA) and recoupled into a multimode fiber. At one end of the multimode fiber, fluorescence photons are detected with a fiber-coupled avalanche photodiode APD1 (SPCM-AQR/FC, PerkinElmer). At the other end of multimode fiber, fluorescence emission spectrum is measured using an optical multichannel analyzer (DV420A-OE, Andor).

Regarding the radiation modes, fluorescence photons are collected by OL, coupled into a multimode fiber by FC3, and detected by a fiber-coupled avalanche photodiode APD2. A set of two filters FL3 (R70/R72, HOYA) is used to reject the scattered laser light from the focus point. Characteristics of APD1 and APD2 are the same, and signals from APD1 and APD2 are accumulated and recorded using photon-counting system (M8784, Hamamatsu). Photon-counting measurements for both guided and radiation modes and spectrum measurements are carried out for each deposited position simultaneously. Additionally, we performed photon-correlation measurements through the guided modes for all deposited positions [17]. All the above fluorescence measurements are carried out for the three nanofiber samples by keeping the excitation laser intensity at a low value of 50 W/cm^2 so that q dots may not deteriorate [18,19].

The channeling efficiency η_c into the nanofiber-guided modes can be expressed as follows:

$$\eta_c = \frac{n_g}{n_g + n_r} = \frac{1}{1 + n_r/n_g}, \tag{1}$$

where n_g and n_r are photon emission rates into the guided and radiation modes, respectively. Observable photon-count rates by APD1 and APD2 are expressed as follows:

$$n_g^{(\mathrm{obs})} = \frac{1}{2}\eta_{\mathrm{APD1}}\kappa_g n_g, \qquad n_r^{(\mathrm{obs})} = \eta_{\mathrm{APD2}}\kappa_r\eta_r n_r, \tag{2}$$

where κ_g and κ_r are light-transmission factors for the paths of guided and radiation modes, respectively. Factor $1/2$ for $n_g^{(\mathrm{obs})}$ corresponds to a fact that fluorescence photons into the guided modes are detected only for one direction of the nanofiber. η_{APD1} and η_{APD2} are the quantum efficiencies of APD1 and APD2, respectively, and are assumed to be the same. η_r is an effective collection efficiency for the radiation modes. Thus, the ratio n_r/n_g can be written as follows:

$$\frac{n_r}{n_g} = \frac{n_r^{(\mathrm{obs})}}{n_g^{(\mathrm{obs})}}\frac{\kappa_g}{2\kappa_r\eta_r} = \frac{n_r^{(\mathrm{obs})}}{n_g^{(\mathrm{obs})}}C, \tag{3}$$

where $C = \kappa_g/2\kappa_r\eta_r$.

κ_g value was measured to be 49.6($\pm$2.1)%. The measurement procedure is as follows: the SLED output is fusion spliced to SMF2 at the FL1 end, and the output power is measured at the APD1 position. Input power to the optical nanofiber is measured by cleaving the SMF1 before entering into the optical nanofiber. The measured value is consistent with a value calculated as a product of transmission factors of optical nanofiber (81%), splicing

point between SMF1 and SMF2 (81%), FL2 (83%), and coupling efficiency into the multimode fiber at FC2 (90%).

The κ_r value was obtained to be 23.5(±1.3)% as a product of transmission factors of all optical components in the path and coupling efficiency into multimode fiber. Transmission factors are measured for OL (74%), beam splitter (63%), flipper mirror (83%), and FL3 (75%) using the SLED light. The coupling efficiency into multimode fiber at FC3 was found to be 81% using the following procedure: First, SLED light is introduced from the LD port and is focused at the nanofiber. The scattered light from the focused spot is collected through the OL, and its power is measured both at FC3 position and at APD2 position through multimode fiber.

Regarding the radiation modes, the effective collection efficiency η_r consists of two factors. One is from NA of the OL. The collection efficiency of the OL is estimated to be 10% from a NA value of 0.6. The other factor arises from the nanofiber itself. The q dots are deposited on the upper surface of nanofiber and the OL collects the fluorescence photons from the downside of nanofiber. Therefore, the nanofiber acts as a cylindrical lens and the collection efficiency of the OL may be enhanced by the lens effect of nanofiber. We calculated the enhancement factor based on the formalism developed in Ref. [20], and estimated the average enhancement factor by assuming random azimuthal distribution of q dots on the upper surface of nanofiber. It was found that the average enhancement factor could be assumed to be constant with a value of 1.48(±0.03) for the fiber diameters of the present measurements. We use this average enhancement factor to obtain the effective collection efficiency η_r. Thus, we obtain the η_r value to be 14.8(±0.3)% and consequently the C value to be 7.13(±0.84) by combining the values of κ_g, κ_r, and η_r.

Figure 2 shows the fluorescence photon-count rate measured for a deposited nanofiber by scanning the focusing point along the nanofiber. The scanning speed is 6 μm/s, and signals are measured through the guided mode by APD1. One can clearly see eight sharp peaks along the nanofiber with a typical separation of 0.5 mm. Origin of the horizontal axis corresponds to the center of the nanofiber. Nanofiber diameter varies from 400 nm at the origin to 750 nm at the position 3.5 mm. Inset shows an expanded profile of a peak marked by an arrow. The width should be limited by the focused spot size on nanofiber and is about 1.5 μm FWHM.

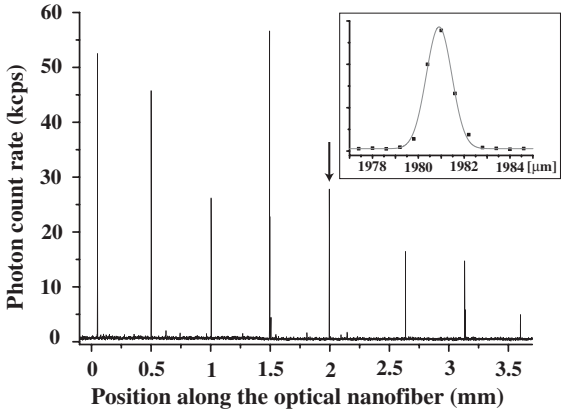

FIG. 2. Observed fluorescence photon-count rate by scanning the focusing point along the nanofiber. Origin of the horizontal axis corresponds to the center of the nanofiber. Inset shows an expanded profile of a peak marked by an arrow. Gray solid curve shows a Gaussian fitting with a width of 1.5 μm FWHM.

Figure 3(a) shows the typical fluorescence photon-count rates from q dots on nanofiber at a fiber diameter of 400 nm. Black (upper) and red (lower) traces correspond to the photon-count rates through the guided and radiation modes, respectively. Measurement time is 5 min with a time bin size of 100 ms. One can readily see that the two traces exactly match with each other. Photon-count rates show a clear single step blinking behavior, revealing that the number of deposited q dots is one. This single q-dot deposition could be further confirmed by measuring the antibunching dip in

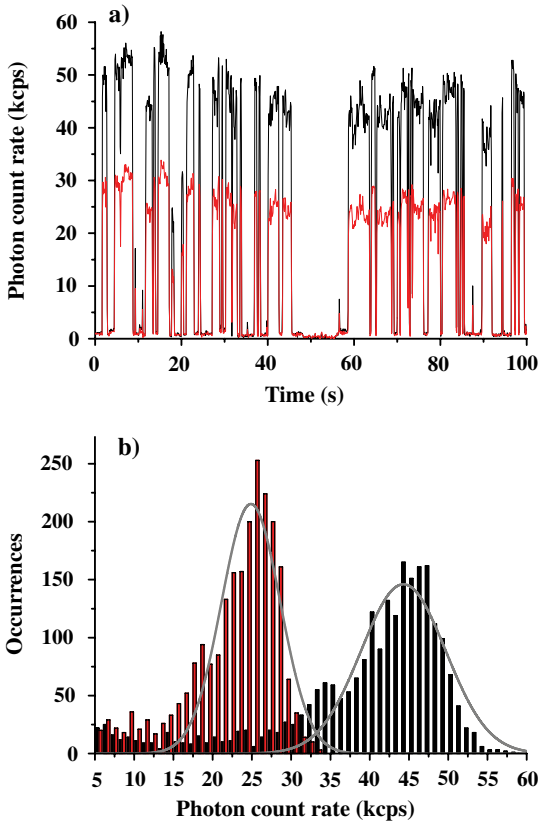

FIG. 3 (color online). (a) Typical fluorescence photon-count rate from a single q dot as a function of time. Black (upper) and red (lower) traces correspond to fluorescence photon-count rates observed through guided and radiation modes, respectively. (b) Histograms for the count rates plotted for guided and radiation modes. The right side black (left side red) histograms correspond to the guided (radiation) modes. Fittings by Gaussian profiles are drawn by gray solid curves. Adjusted R^2 for the fittings are estimated to be 0.85 and 0.86 for the right side black and left side red histograms, respectively.

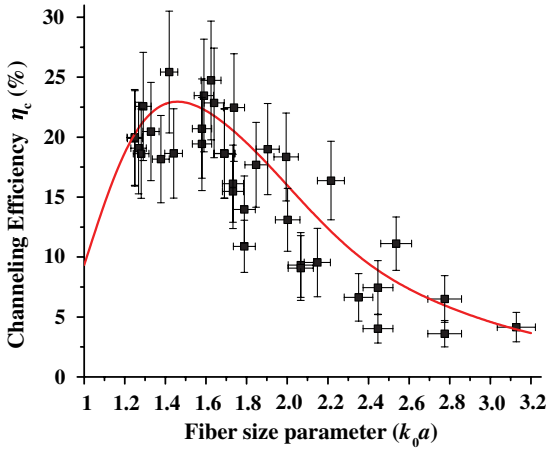

FIG. 4 (color online). Channeling efficiency as a function of fiber size parameter ($k_0a = 2\pi a/\lambda$). Red solid curve denotes the theoretical prediction. Measured values are marked by black squares with error bars.

the normalized photon correlations, and the dip value was measured to be $0.035 \ll 1$. The above measurements were performed for the three nanofiber samples for all the depositions, and the number of q dots at each deposition was measured to be one or two, similarly as in Ref. [17]. Regarding the fluorescence spectrum, the center wavelength distributes over the range of 80 nm from 740 to 820 nm with a typical FWHM of 52 nm.

Figure 3(b) shows the photon-count rate histograms for the black and red traces for the whole measurement time with a counting interval of 1 kcps. The two histograms reveal good matching with each other. One can recognize a small peak on the tail of histograms. Such a peak may imply the existence of weaker emission levels for the q dot as discussed in Ref. [21]. By fitting the histograms with Gaussian profiles [19], we obtain $n_g^{(\mathrm{obs})}$ and $n_r^{(\mathrm{obs})}$ to be 44.3($\pm$5.4) and 24.8($\pm$3.7) kcps, respectively. Using the relation of Eq. (3), the ratio n_r/n_g is obtained to be 3.99($\pm$1.55). Thus, using Eq. (1) we obtain the η_c value to be 20.0($\pm$6.2)%. Using the same procedure, the η_c values were obtained at various fiber diameters for the three nanofiber samples.

Figure 4 shows the channeling efficiency η_c as a function of fiber size parameter ($k_0a = 2\pi a/\lambda$). The size parameter is calculated for each deposited position by using the measured fiber diameter $2a$ and the observed emission wavelength λ. The red curve exhibits the theoretical prediction for the channeling efficiency into the HE_{11} mode assuming the nanofiber refractive index of 1.45. All measured values are plotted against size parameter as black squares. Vertical error bars are due to the fluctuation of photon counts at each deposited position, as shown in Figs. 3(a) and 3(b). Horizontal error bars are due to the ambiguity in fiber-diameter measurements. Regarding the fluctuation of black squares, the main origin would be measurement ambiguity, but ambiguity of the enhancement factor for the nanofiber lens effect would also be another origin. For the experimental analysis, we used the average enhancement factor assuming random azimuthal distribution of deposition, but the enhancement factor for each deposited position would be different from the average value. Such ambiguity should induce the fluctuation to the obtained η_c values. Although experimental ambiguities still exist, it should be mentioned that the measured results have reproduced the theoretical prediction within the experimental ambiguities. We have estimated the maximum channeling efficiency into the guided modes to be 22.0($\pm$4.8)%, by averaging for data points around the fiber size parameter of 1.4, which corresponds to the fiber diameter of 350 nm for the emission wavelength of 780 nm.

In conclusion, we have experimentally demonstrated the efficient channeling of fluorescence photons from single q dots on optical nanofiber into the guided modes, by measuring the photon-count rates through the guided and radiation modes simultaneously. We have obtained the maximum channeling efficiency of 22.0($\pm$4.8)% around the fiber size parameter of 1.4, as theoretically predicted [5,6]. We should note that the present results may open a way to realize the channeling efficiency higher than 90%, by incorporating cavity structure on nanofiber [22,23]. Such nanofiber-cavity system combined with advanced quantum emitters, like unblinking color centers in nanodiamonds [24,25], may lead to a new route to the on-demand single-photon generation into single-mode optical fibers.

We thank Kali Nayak for helpful discussions. This work was carried out as a part of the Strategic Innovation Project by Japan Science and Technology Agency.

[1] G. S. Solomon, M. Pelton, and Y. Yamamoto, Phys. Rev. Lett. **86**, 3903 (2001).
[2] G. Shambat, J. Provine, K. Rivoire, T. Sarmiento, J. Harris, and J. Vuckovic, Appl. Phys. Lett. **99**, 191102 (2011).
[3] T. Schroder, F. Gadeke, M. J. Banholzer, and O. Benson, New J. Phys. **13**, 055017 (2011).
[4] A. V. Akimov, A. Mukherjee, C. L. Yu, D. E. Chang, A. S. Zibrov, P. R. Hemmer, H. Park, and M. D. Lukin, Nature (London) **450**, 402 (2007).
[5] V. V. Klimov and M. Ducloy, Phys. Rev. A **69**, 013812 (2004).
[6] F. Le Kien, S. Dutta Gupta, V. I. Balykin, and K. Hakuta, Phys. Rev. A **72**, 032509 (2005).
[7] K. P. Nayak, P. N. Melentiev, M. Morinaga, F. Le Kien, V. I. Balykin, and K. Hakuta, Opt. Express **15**, 5431 (2007).
[8] A. Stiebeiner, R. Garcia-Fernandez, and A. Rauschenbeutel, Opt. Express **18**, 22677 (2010).
[9] K. P. Nayak and K. Hakuta, New J. Phys. **10**, 053003 (2008).
[10] K. P. Nayak, F. Le Kien, M. Morinaga, and K. Hakuta, Phys. Rev. A **79**, 021801(R) (2009).

[11] M. Das, A. Shirasaki, K. P. Nayak, M. Morinaga, F. Le Kien, and K. Hakuta, Opt. Express **18**, 17154 (2010).
[12] V. I. Balykin, K. Hakuta, F. Le Kien, J. Q. Liang, and M. Morinaga, Phys. Rev. A **70**, 011401(R) (2004).
[13] F. Le Kien, V. I. Balykin, and K. Hakuta, Phys. Rev. A **70**, 063403 (2004).
[14] G. Sagué, A. Baade, and A. Rauschenbeutel, New J. Phys. **10**, 113008 (2008).
[15] E. Vetsch, D. Reitz, G. Sague, R. Schmidt, S. T. Dawkins, and A. Rauschenbeutel, Phys. Rev. Lett. **104**, 203603 (2010).
[16] M. Fujiwara, K. Toubaru, T. Noda, H. Q. Zhao, and S. Takeuchi, Nano Lett. **11**, 4362 (2011).
[17] R. R. Yalla, K. P. Nayak, and K. Hakuta, Opt. Express **20**, 2932 (2012); arXiv:1112.0624v1.
[18] T. Ota, K. Maehashi, H. Nakashima, K. Oto, and K. Murase, Phys. Status Solidi B **224**, 169 (2001).
[19] K. Goushi, T. Yamada, and A. Otomo, J. Phys. Chem. C **113**, 20161 (2009).
[20] J. A. Stratton, *Electromagnetic Theory* (McGraw-Hill, New York, 1941), details will be reported elsewhere.
[21] B. R. Fisher, H. J. Eisler, N. E. Stott, and M. G. Bawendi, J. Phys. Chem. B **108**, 143 (2004).
[22] F. Le Kien and K. Hakuta, Phys. Rev. A **80**, 053826 (2009).
[23] K. P. Nayak, F. Le Kien, Y. Kawai, K. Hakuta, K. Nakajima, H. T. Miyazaki, and Y. Sugimoto, Opt. Express **19**, 14040 (2011).
[24] I. Aharonovich, S. Castelletto, D. A. Simpson, C.-H. Su, A. D. Greentree, and S. Prawer, Rep. Prog. Phys. **74**, 076501 (2011).
[25] E. Neu, D. Steinmetz, J. Riedrich-Moller, S. Gsell, M. Fischer, M. Schreck, and C. Becher, New J. Phys. **13**, 025012 (2011).